

Evaluation of a Direct Air Capture Process Combining Wet Scrubbing and Bipolar Membrane Electrodialysis

Francesco Sabatino, Mayank Mehta, Alexa Grimm, Matteo Gazzani, Fausto Gallucci, Gert Jan Kramer, and Martin van Sint Annaland*



Cite This: *Ind. Eng. Chem. Res.* 2020, 59, 7007–7020



Read Online

ACCESS |



Metrics & More

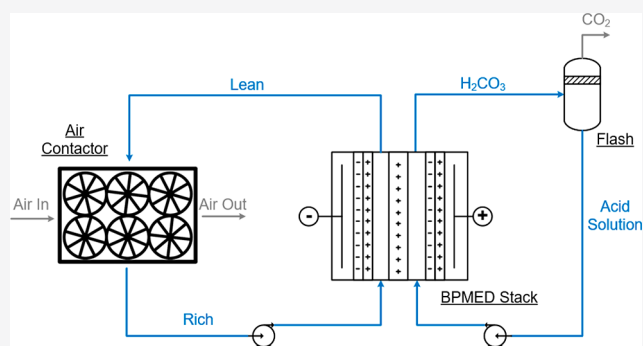


Article Recommendations



Supporting Information

ABSTRACT: A detailed techno-economic analysis of a novel direct air capture (DAC) process has been carried out. In this process, carbon dioxide is separated from ambient air through wet scrubbing with an aqueous potassium hydroxide solution, while the solvent regeneration and CO₂ recovery is carried out through bipolar membrane electrodialysis (BPMED), a novel process exclusively based on electrical-driven regeneration. The results of the techno-economic analysis showed that the regeneration process could be less energy intensive than other solutions, requiring as low as 236 kJ/mol-CO₂. However, the high costs of bipolar and ion exchange membranes make the BPMED expensive. In the base-case scenario, the total capture cost has been found to be 773 \$/ton-CO₂, in line with previous cost estimates for DAC but large for a second generation process. As for other DAC processes, this solution could become particularly interesting in the future, whenever cheaper renewable energy and more affordable and improved membranes become available.



1. INTRODUCTION

Anthropogenic CO₂ emissions have already caused an increase in the global temperature of 1 °C above pre-industrial levels, with clear consequences for our planet, such as rising sea levels, decline in arctic ice, and growing frequency of extreme weather events. To reduce the impact of climate change, the governments of 195 countries have adopted in 2015 the Paris Climate Agreement, pledging to limit the temperature increase to 1.5 °C. Achieving this objective will not be an easy task, as it will require a drastic reduction in CO₂ emissions by 2030 and net zero emissions by 2050.¹ However, at the moment, global emissions of carbon dioxide are still increasing. It should not come as a surprise, then, that most of the pathways consistent with a maximal 1.5 °C temperature increase depend on large-scale removal of CO₂ from the atmosphere.

A few negative emissions technologies (NETs) have been proposed, and direct air capture (DAC) is the one with the largest potential.² DAC refers to a process for separating carbon dioxide from ambient air, a concept first proposed by Lackner et al. in 1999.³ Although Lackner was the first to suggest the deployment of such a process to mitigate climate change, technologies for the extraction of CO₂ from air have been used since the 1950s in closed-circuit breathing systems found in submarines and spaceships.⁴ DAC is not only technologically possible but also from a thermodynamic perspective it does not require much more energy than

separating carbon dioxide from concentrated sources such as flue gases.⁵

Extracting CO₂ from such a diluted source has, of course, its drawbacks. Large volumes of air have to be processed to capture a meaningful amount of CO₂. As an example, a DAC plant with a capture rate of 1 Mton-CO₂/yr would need to process at least 46,000 m³/s of air. This requirement places severe constraints on the capture process itself. Indeed, physical separation processes are probably doomed to be economically unfeasible, as the energy requirements to change the temperature and pressurize such a diluted stream as air would be prohibitively high.⁶ Although other methods could be possible, most of the research published in the literature and the processes developed follow the same approach, that is, sorption of CO₂ with a liquid or solid material. The adsorption route is probably the most studied:⁷ different classes of solid sorbents have been proposed in the literature, with metal–organic frameworks (MOFs),⁸ supported amines,⁹ and solid alkali carbonates¹⁰ being the most prominent. On the other hand, the wet scrubbing technology is more mature.

Special Issue: Carbon Capture and Utilization

Received: October 16, 2019

Revised: January 14, 2020

Accepted: January 14, 2020

Published: January 15, 2020



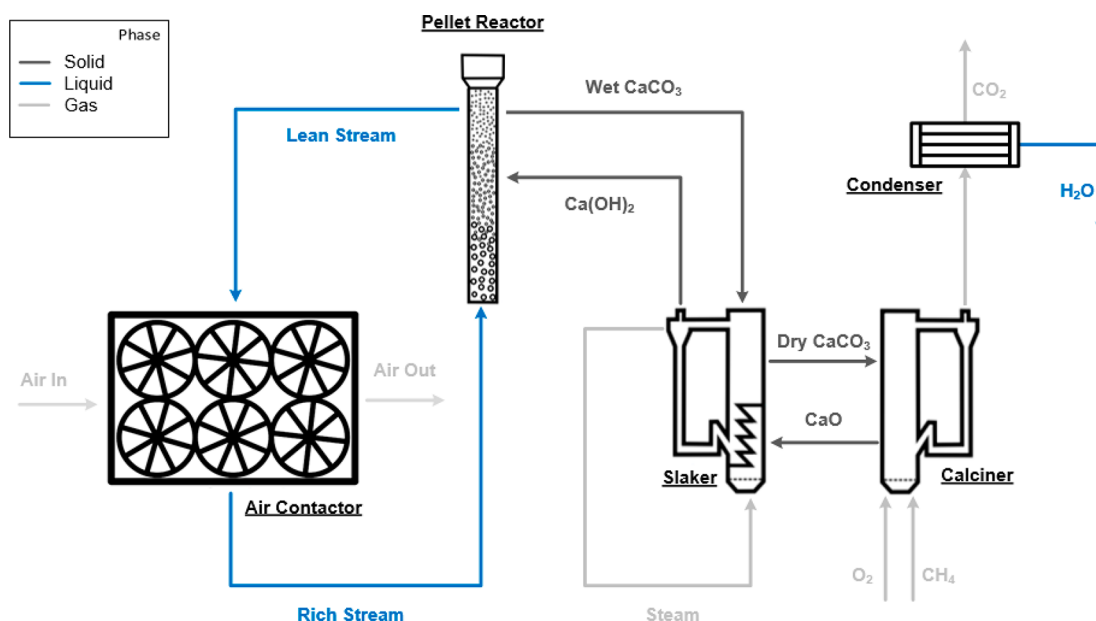


Figure 1. Simplified flowsheet of Carbon Engineering DAC process.

In the process described by Lackner,¹¹ CO₂ is separated from air by an aqueous sodium hydroxide solution, which is subsequently regenerated through a complex and energy-intensive calcium-based thermochemical cycle derived from the pulp and paper industry.¹² This concept was further developed by Baciocchi et al.,¹³ providing the first design of a DAC system on the grounds of mass and energy balances. Based on these results, the American Physical Society (APS) estimated the cost of such a process to be 600 \$/ton-CO₂.¹⁴ In parallel, the concept was further improved by David Keith, one of the founders of the Canadian-based DAC company Carbon Engineering (CE). The most recent cost estimate provided by Keith is 94–232 \$/ton-CO₂,¹⁵ roughly a factor 3–6 lower than the APS assessment. The drastic cost reduction was made possible by careful design choices and rigorous optimization.

The complex calcium-based thermochemical cycle is not the only option for the regeneration of the hydroxide solvent. Indeed, several technologies for the desorption of carbon dioxide from alkaline solutions have been described in the literature.¹⁶ Among these, bipolar membrane electrodialysis (BPMED) is particularly interesting, as it is an entirely electric process which could be powered only with renewable energy sources. As the regeneration too is carried out in the liquid phase, this technology has also the additional benefit of avoiding phase transitions and solids handling.

With BPMED, CO₂ is recovered from rich streams through ion transport across membranes driven by a difference in electric potential. Different cell configurations can be arranged, depending on the number and the kind of membrane chosen. The simplest cell structure consists of a bipolar membrane (BPM), whose role is to split water in H⁺ and OH[−] ions, and an ion-exchange membrane. Carbon dioxide is present in the system in the form of bicarbonate (HCO₃[−]) and carbonate (CO₃^{2−}) anions, which are converted to CO₂ via H⁺ ions separated in the BPM.

Recently, BPMED has found several industrial applications, such as production of ultrapure deionized water, pH correction processes in chemical solutions, and production of organic and inorganic acids and bases from their respective salts.¹⁷

Although not yet deployed at industrial or even pilot scale, CO₂ separation through BPMED has been already described in the literature.

Nagasawa et al. investigated the effect of different cell configurations on the carbon dioxide recovery from sodium bicarbonate solutions.¹⁸ The energy demand of a BPMED process is strongly influenced by the membrane arrangement in the cell and the distance between adjacent membranes. Nagasawa observed that a two-compartment configuration using a BPM and a cation-exchange membrane (CEM) was the most efficient, requiring 2.1 MJ/kg-CO₂ for the solvent regeneration. Building on this work, Iizuka et al. assessed the effect of the major operating conditions on the performance of the processes using commercially available electrodialysis equipment.¹⁹ Iizuka and co-workers also provide a rough cost estimate for a postcombustion CO₂ capture process consisting of wet scrubbing of flue gas in a packed tower with an aqueous solution of sodium hydroxide and subsequent regeneration of the solvent through BPMED. Through optimization of the operating conditions, a minimum cost of 180 \$/ton-CO₂ was achieved.

Eisaman et al. investigated experimentally the application of BPMED for the regeneration of CO₂-rich potassium carbonate and bicarbonate solutions.²⁰ This work is of particular interest since it provides the performance of this process using six different mixtures of KOH, K₂CO₃, and KHCO₃. The results showed that the composition of the rich stream has a great influence on the efficiency of the CO₂ recovery. The presence of residual potassium hydroxide in the rich stream hinders the efficiency of the BPMED process significantly, a phenomenon that is considered and dealt with in this work. Eisaman also observed that the release of the dissolved CO₂ could take place almost immediately in the membrane stack, thus impairing the conduction of electrical current. A solution to this problem was proposed and assessed experimentally in a subsequent work.²¹ Since the amount of gas dissolved in a liquid increases with increasing pressure, by operating the entire stack at sufficiently high pressures, the formation of CO₂ bubbles in the stack can be avoided. This proved to be expedient, as it provided a

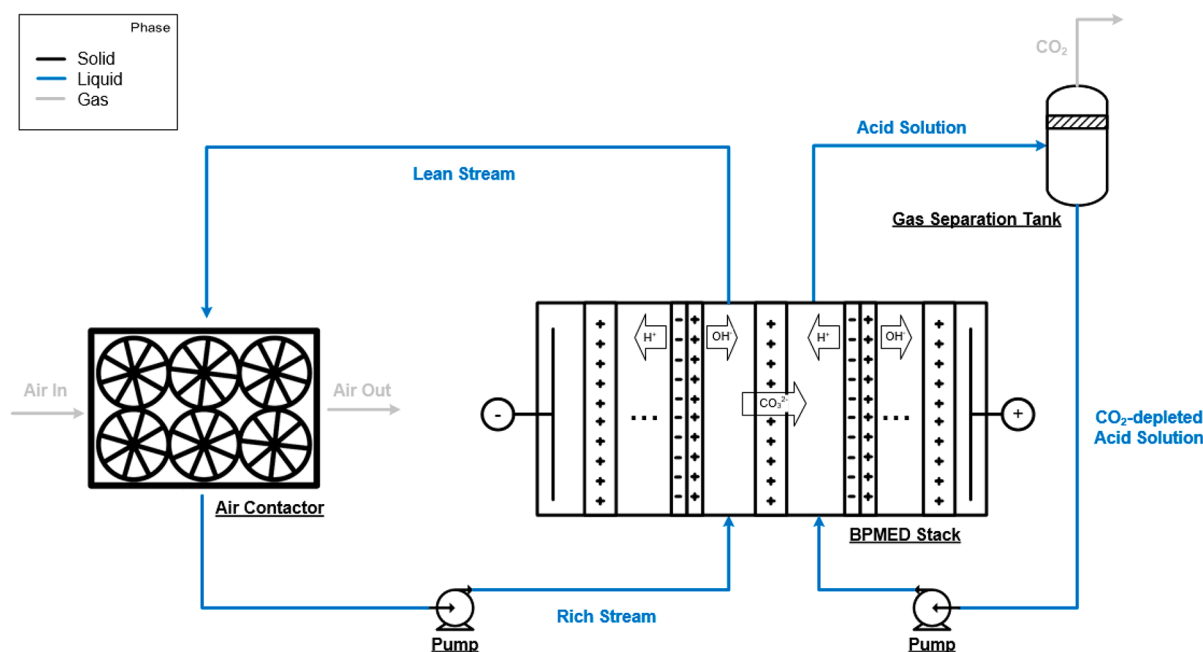


Figure 2. Schematic representation of the proposed WS-BPMED DAC process.

reduction in the energy demand up to 29% by operating at pressures above 6 atm. The carbon dioxide is eventually recovered through depressurization after electrodialysis. Eisaman et al. also proposed another interesting NET based on BPMED, namely, the extraction of CO_2 from seawater.²² This process would separate carbon dioxide from the atmosphere without the need to process large volumes of air.

Although electrodialysis has been proposed for application in a DAC process²³ and it has been assessed for CO_2 release in a postcombustion application,¹⁹ no techno-economic analysis of a DAC process combining wet scrubbing and solvent regeneration technology based on BPMED has been reported in the open literature yet. With this work, we aim at filling in this gap.

The process we investigate adopts the optimized air contactor unit developed by Carbon Engineering. We first aim at providing a detailed process analysis and proving the conceptual validity of the process. Since the effectiveness of the CO_2 capture depends on the performance of the sorbent regeneration and vice versa, modeling of the entire process is required to provide an accurate evaluation. The simulation and optimization of the capture process have been carried out in Aspen Plus. A detailed flowsheet of the air contactor has been developed based on extensive data published by Carbon Engineering.²⁴ The BPMED unit is modeled in MATLAB. Experimental results published by Eisaman et al.²⁰ are used to validate the model. These tools have been used to assess and improve the process performances through sensitivity analysis and process optimization. Finally, an economic assessment has been carried out. Sensitivity analyses are used to assess which are the most influential parameters.

2. PROCESS DESCRIPTION

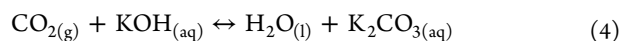
2.1. Carbon Engineering Process. The Carbon Engineering process, which is schematically represented in Figure 1, is described below.

Ambient air is fed to the air contactor unit, where it is contacted with an aqueous solution of potassium hydroxide.

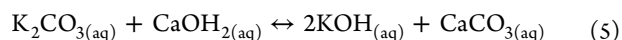
Alkali hydroxides have strong CO_2 -binding affinities and are thus capable of capturing carbon dioxide from air. The mechanism of CO_2 absorption in hydroxide solutions is well known. At pH greater than 10, the predominant reactions are as follows:²⁵



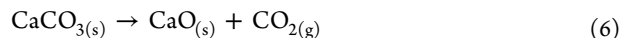
The overall reaction is



The CO_2 -rich capture solution is then fed to the pellet reactor, in which it is regenerated through causticization with lime, i.e., $\text{Ca}(\text{OH})_2$, according to the following reaction:

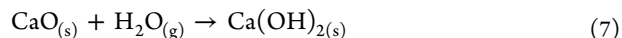


Due to its extremely low solubility in water, calcium carbonate precipitates and is easily separated from the capture solution, which is sent back to the air contactor. Wet CaCO_3 particles are initially dried in the steam slaker and subsequently fed to the calciner, where calcination takes place



Calcination is a highly endothermic process requiring a temperature of 900 °C. These substantial energy requirements are met through oxyfuel combustion of methane.

The final step is the hydration of CaO to $\text{Ca}(\text{OH})_2$, a process known as slaking



The slaker differs from the conventional ones used in the Kraft process, as it is operated with steam at a temperature of 300 °C. This design choice allows for the release of the enthalpy of the slaking reaction (eq 7) at higher temperatures, while at the same time achieving fast kinetics.

Compared to similar processes,^{13,26} the air contactor is certainly the component that most required dedicated development to be able to handle large air flow rates.^{27,28} As stated before, it is of paramount importance to put the sorbent and air in contact in the most efficient way. The Carbon Engineering contactor is based on the same technology used in cooling towers, which are designed to efficiently bring ambient air in contact with a fluid. CE, however, adopted a cross-flow configuration: air flows horizontally while the capture solution flows downward on plastic structured packing. CE's air contactor is essential in bringing down the cost of DAC. Indeed, the cost estimated by the APS for the capture alone of CO₂ with a conventional counter-flow gas scrubber column is 240 \$/ton-CO₂, roughly a factor of 4 higher than what CE expects.²⁷

The process developed by CE has the advantage of being based on mature, well-established technologies. The version described above, however, is far from being the final one. It is, indeed, expected that several improvements will be implemented as the first plants are built and the process is further optimized, especially to avoid the use of natural gas. Moreover, CE is also developing alternative processes based on the same air contactor design.²⁹

2.2. BPMED Regeneration Process. The wet scrubbing-BPMED (WS-BPMED) process is schematically represented in Figure 2. CO₂ is extracted from air through wet scrubbing with an aqueous solution of KOH in a cross-flow absorption unit as designed by Carbon Engineering.²⁸ As described earlier, potassium hydroxide reacts with carbon dioxide to produce K₂CO₃ and KHCO₃, which in water are present as K⁺ cations and CO₃²⁻/HCO₃⁻ anions.

The rich stream is fed to a BPMED stack for regeneration. A two-cell configuration has been selected, consisting of a BPM and an anion exchange membrane (AEM), which divides the cell into an acidic and a basic compartment, as shown in Figure 3. The rich stream flows in the basic compartment, while in the

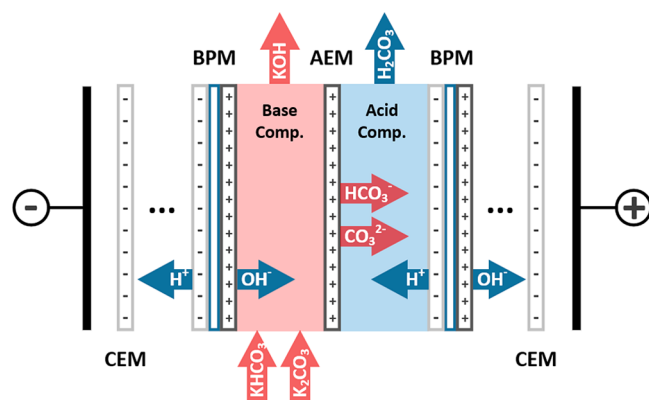
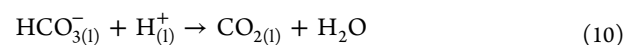


Figure 3. Configuration of the two-compartment BPMED cell (AEM = anion exchange membrane; CEM = cation exchange membrane; BPM = bipolar membrane).

acid compartment a buffer solution is fed. BPMs are bilayer structures composed of cation-exchange and anion-exchange layers possessing ion-selective properties. When an electric current is passed through them, BPMs split water in H⁺ and OH⁻, provided that the potential is higher than the one necessary for water dissociation. In the base compartment, the K⁺ and OH⁻ ions react to form KOH.



The CO₂-carrying ions diffuse through the AEM to the acid compartment, where they react with H⁺ to produce dissolved carbon dioxide.



Since the solubility of carbon dioxide in the acid solution is extremely small, most of the CO₂ is immediately released in the form of bubbles. This can prove to be quite problematic since bubbles could cause an increase in the electrical resistance of the cell, thus increasing the energy demand of the process.

The regenerated lean solution is fed back to the air contactor, while the biphasic acid solution is sent to a vessel to separate the gaseous CO₂ from the acid buffer solution. The pure carbon dioxide is finally compressed to 150 bar in a multistage compressor.

3. METHODOLOGY

3.1. Air Contactor Flowsheet. The air contactor unit has been modeled in Aspen Plus. The thermodynamics of the absorption process are quite complex since they involve physical and chemical equilibria of an electrolyte system. Accordingly, we make use of the ELECNRTL property method.

The air contactor has been modeled in detail based on the several contributions published by Carbon Engineering.^{15,27,28} The cross-flow design has been reproduced by implementing several rate-based RADFRAC units to simulate packed compartments.

The ionic reactions which describe the CO₂ absorption mechanism (eqs 1, 2, and 3) have been modeled through a chemistry model with chemical equilibrium reactions. Moreover, a kinetic reaction model has also been implemented for the rate-based calculations carried out in the RADFRAC blocks. More details can be found in the Aspen documentation.³⁰

3.2. BPMED Model. The total costs of the BPMED process are given by the membrane area requirement and by the power consumption.³¹ The necessary membrane area can be estimated from the molar flux of CO₃²⁻ and HCO₃⁻ ions, *J* (mol m⁻² s⁻¹), which can be expressed with eq 11

$$J = \frac{iS}{F}\eta \quad (11)$$

where *S* (m²) is the area of a single membrane, *F* (A s mol⁻¹) is the Faraday constant, *i* (A m⁻²) is the current density, and *η* is the current efficiency, defined as the ratio between the number of moles of CO₂ transported across the AEM over the charge transported. According to this definition, the maximum achievable efficiency is equal to 1 for solutions containing exclusively KHCO₃ (since HCO₃⁻ carries a single charge) and 0.5 for solutions of K₂CO₃ (as in this case the charges would be transported by CO₃²⁻ ions). The efficiency, therefore, gives a measure of which ions are being transported, as the transfer of CO₂-free ions (i.e., OH⁻) will reduce *η* from the maximum value.

The power consumption, on the other hand, depends on the voltage drop across the BPMED cell, which is given by eq 12

$$E_{\text{cell}} = iR_{\text{cell}} + E_{\text{BP}} \quad (12)$$

where R_{cell} ($\Omega\text{m}^2/\text{cell}$) is the electrical resistance of a unit area of a single cell, and E_{BP} (V) is the water-splitting potential of the BPM. The total cell resistance is given by the sum of the individual solutions (acid and base) and membrane resistances

$$R_{\text{cell}} = R_{\text{base}} + R_{\text{AEM}} + R_{\text{acid}} \quad (13)$$

The resistance of the solutions is calculated with the following expression

$$R_{\text{solution}} = \frac{\delta}{k_{\text{solution}}} \quad (14)$$

with δ (m) the distance between the BPM and the AEM. The electrical conductivity of the acid solution k_{solution} is not assumed to be constant and is corrected to account for the formation of gaseous CO_2 . Indeed, due to its low solubility in the acidic solution, most of the dissolved carbon dioxide is released in the form of bubbles. The presence of gas bubbles determines a reduction of the electrical conductivity, which is described with eqs 15 and 16³²

$$\frac{k_{\text{acid}}^*}{k_{\text{acid}}} = \frac{1 + AB\varphi_{\text{CO}_2}}{1 - B\gamma\varphi_{\text{CO}_2}} \quad (15)$$

$$\gamma = 1 + \frac{1 - \varphi_m}{\varphi_m^2} \varphi_{\text{CO}_2} \quad (16)$$

where A and B are parameters which depend on the shape of the bubbles and their conductivity (assumed to be zero), φ_{CO_2} is the volumetric fraction of CO_2 bubbles in the acid solution, and φ_m is the maximum achievable volumetric fraction.

The power consumption of a single cell P_{cell} (W/cell) is then calculated with eq 17

$$P_{\text{cell}} = iSE_{\text{cell}} \quad (17)$$

And, finally, the specific energy demand (kJ/mol- CO_2) is given by

$$\text{SPEND} = \frac{N_{\text{stack}} N_{\text{cell}} P_{\text{cell}}}{J} \quad (18)$$

From eq 11, it can be inferred that the required membrane area S is inversely proportional to the current density i for constant product rate J and current efficiency η . This implies that the number of membranes, i.e., the capital costs, decreases with increasing current density. However, from eq 17, it is clear that the power consumption, which is closely related to the operating costs, increases with i . Therefore, an optimal current density can be found, for which the total cost of the BPMED process will be the lowest.

3.4. BPMED Efficiency. The current efficiency depends on several parameters, including the properties of the BPM and the composition of acidic and basic solutions.³¹ Due to the complex nature of this parameter, it is usually measured experimentally.

In this work, experimental data provided by Eisaman et al.²⁰ has been used to determine the current efficiency η . Eisaman et al. carried out experiments in a lab-scale setup consisting of seven cells in series, each containing an AEM and a BPM. The performances of this system have been assessed with eight different mixtures of KOH, K_2CO_3 , and KHCO_3 . The measured and fitted current efficiencies for the eight solutions are reported in Figure 4.

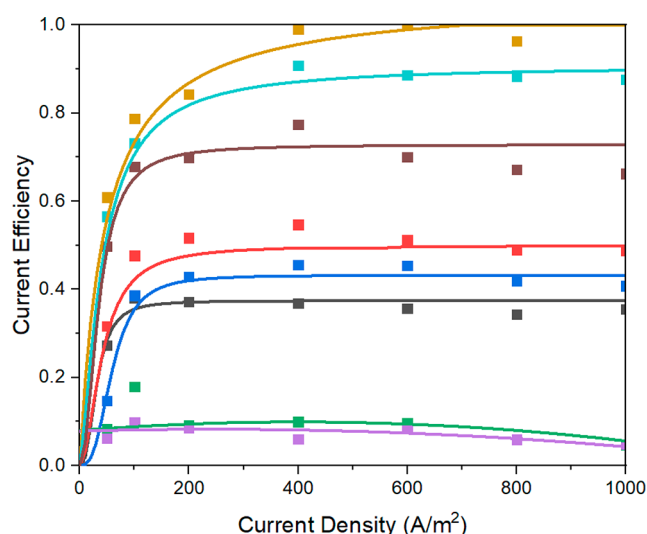


Figure 4. Current efficiency (squares) measured experimentally²⁰ and fitted current efficiency (lines) (eq 19) for (black) 0.125 M K_2CO_3 , (red) 0.5 M K_2CO_3 , (dark blue) 2 M K_2CO_3 , (light blue) 0.25 M K_2CO_3 + 0.25 M KHCO_3 , (brown) 0.375 M K_2CO_3 + 0.125 M KHCO_3 , (yellow) 0.5 M KHCO_3 , (green) 0.5 M K_2CO_3 + 0.1 M KOH, and (purple) 0.5 M K_2CO_3 + 0.5 M KOH-rich solutions.

As explained previously, by definition the maximum achievable efficiency for a solution containing exclusively K_2CO_3 or KHCO_3 is, respectively, 0.5 and 1. The presence of KOH in the rich stream strongly affects the efficiency, as OH^- ions will also be transported without contributing to the release of CO_2 .

As a function of current density, the experimental data shows the same behavior. The efficiency is initially very low but reaches a somewhat constant value at higher i . A good fit has been achieved with eq 19, as observable in Figure 4.

$$\eta = \frac{\eta_c k i^{1/m}}{1 + k i^{1/m}} \quad (19)$$

where η_c represents the asymptotic value reached by the efficiency at high current densities and k and m are fitting parameters. Their values for the different rich solution compositions are reported in Table S2 in the Supporting Information. Jorissen and Simmrock reported that the dependence of the current efficiency on the current density is determined by the relative concentration of H^+ and OH^- ions in the acid and basic compartments on either side of the AEM.³³ Indeed, for low values of i , the H^+ concentration in the acid solution is much greater than the OH^- concentration, meaning that the AEM is in the acidic state, and co-ion leakage of H^+ through the membrane is likely to take place. However, the effect of H^+ leakage decreases with increasing current density.

For the solutions containing KOH, however, the current efficiency shows a weak dependence on the current density. In these cases, a second-order polynomial provided the best fit for η .

Figure 4 also shows that the concentration of the electrolyte component has an influence on the efficiency. Indeed, it is possible to observe that η initially increases with increasing K_2CO_3 concentration from 0.125 to 0.5 M and eventually decreases for the highest concentration of 2 M. According to Eisaman et al.,²⁰ this behavior is associated with differences in

pH of the three carbonate solutions, resulting in different OH^- concentrations. This phenomenon is further examined with the help of the Aspen Plus thermodynamic model.

3.5. Economic Analysis. To assess whether the BPMED regeneration does indeed provide an improvement over the thermochemical cycle, an economic assessment has been carried out. The comparison between the two routes has been carried out on the grounds of the capture cost, which is defined as follows:

$$\text{Capture cost} = \frac{(\text{TOC} \times \text{CCF}) + C_{\text{O\&M}}^{\text{fix}} + (C_{\text{O\&M}}^{\text{var}} \times h_{\text{eq}})}{F_{\text{CO}_2}^{\text{BPMED}} \times h_{\text{eq}}} \quad (20)$$

where TOC is the total overnight capital defined in accordance with NETL guidelines³⁴ and is calculated as reported in Table 1. This procedure is based on a bottom up approach in which

Table 1. Methodology for Calculation of TOC³⁴

Bare Erected Cost [BEC]	BEC
Direct costs as a percentage of EC (includes piping/valves, civil works, instrumentation, steel structure, etc.)	
Total installation cost [TIC]	80% BEC
Total direct plant cost [TDPC]	BEC + TIC
Indirect costs [IC]	13% TDPC
Engineering, procurement, and construction [EPC]	TDPC + IC
Contingencies and owner's cost	
Contingency	25% EPC
Owner's cost	5% EPC
Total contingencies and owner's cost [C&OC]	30% EPC
Total overnight capital [TOC]	EPC + C&OC

the cost of the plant is the sum of the cost of the single units, plus direct and indirect costs. Since the TOC represents the overall capital expenditure save the interest incurred during construction of the plant, for the calculation of the capture cost, the capital charge factor (CCF) is also used. Both escalation and interest took out during construction are included in the CCF. The actual value of the CCF depends on the financing method adopted for the project and several financial parameters. We have assumed a value of 12.5%, the same value adopted by Keith et al. for their assessment of Carbon Engineering's process.¹⁵

Operation and maintenance costs ($C_{\text{O\&M}}$) are divided into fixed costs ($C_{\text{O\&M}}^{\text{fix}}$), which account for maintenances, wages,

insurance, and membrane replacement, and variable costs ($C_{\text{O\&M}}^{\text{var}}$), which are related to the cost of water and electricity. The plant availability, which affects the equivalent working hours (h_{eq}), has been assumed to be 90%.

4. RESULTS

Following the methodology described in the previous section, a techno-economic evaluation of the proposed WS-BPMED process is carried out. The BPMED model, validated with experimental data published in the literature, is used to assess the performances and the costs of an industrial-scale unit. Optimization of the operating conditions is achieved by combining the results provided by the BPMED model with simulations of the air contactor carried out in Aspen Plus. Finally, the WS-BPMED process is compared with the benchmark absorption technology in the DAC field, that is, CE process.

4.1. BPMED Model Validation. Eisaman et al.²⁰ calculated the current efficiency η by measuring the CO_2 gas generation rate and the energy consumption for a wide range of current densities. These data have been used to validate the BPMED model. The properties of membranes and electrolytic solutions needed in the model have been collected from the literature or vendor catalogues and are reported in the Supporting Information.

As explained previously, an equation for the current efficiency was obtained by fitting of experimental data. The result for a rich solution containing 0.125 M K_2CO_3 is reported in Figure 5a. Once η is known, the CO_2 production rate can be calculated with eq 11. Figure 5b shows that a good description is achieved. Finally, the specific energy demand is estimated with eq 18. The model, as presented in Figure 5c, provided adequate results, with a maximum error of 12% compared to the experimental value.

The results obtained for the CO_2 production rate for different solutions are reported in Figure 6. It can be observed that the model provides good results across all the rich compositions. As the flux of CO_2 -carrying ions is proportional to η (eq 11), the higher the current efficiency is, the steeper the CO_2 production rate curve is. Therefore, solutions of KHCO_3 (Figure 6c–e) show the fastest rate, as they offer the highest efficiency. On the other hand, in the case of a solution containing an initial concentration of KOH , such as the one reported in Figure 6f, the production rate of carbon dioxide is extremely slow.

Figure 7 shows a comparison between the specific energy demand measured by Eisaman et al.²⁰ and the model results. Also, in this case, the model was able to adequately reproduce

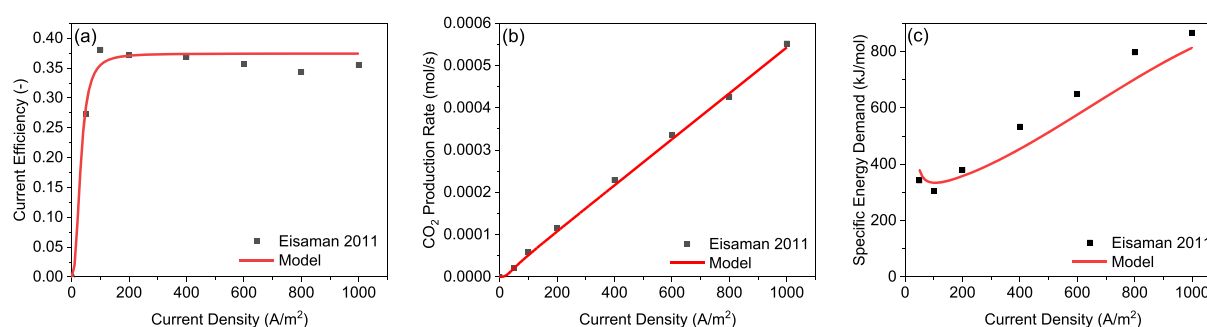


Figure 5. (a) Current efficiency, (b) CO_2 production rate, and (c) specific energy demand as a function of current density (black square) measured experimentally²⁰ and (red line) calculated with the BPMED model for a 0.125 M K_2CO_3 -rich solution.

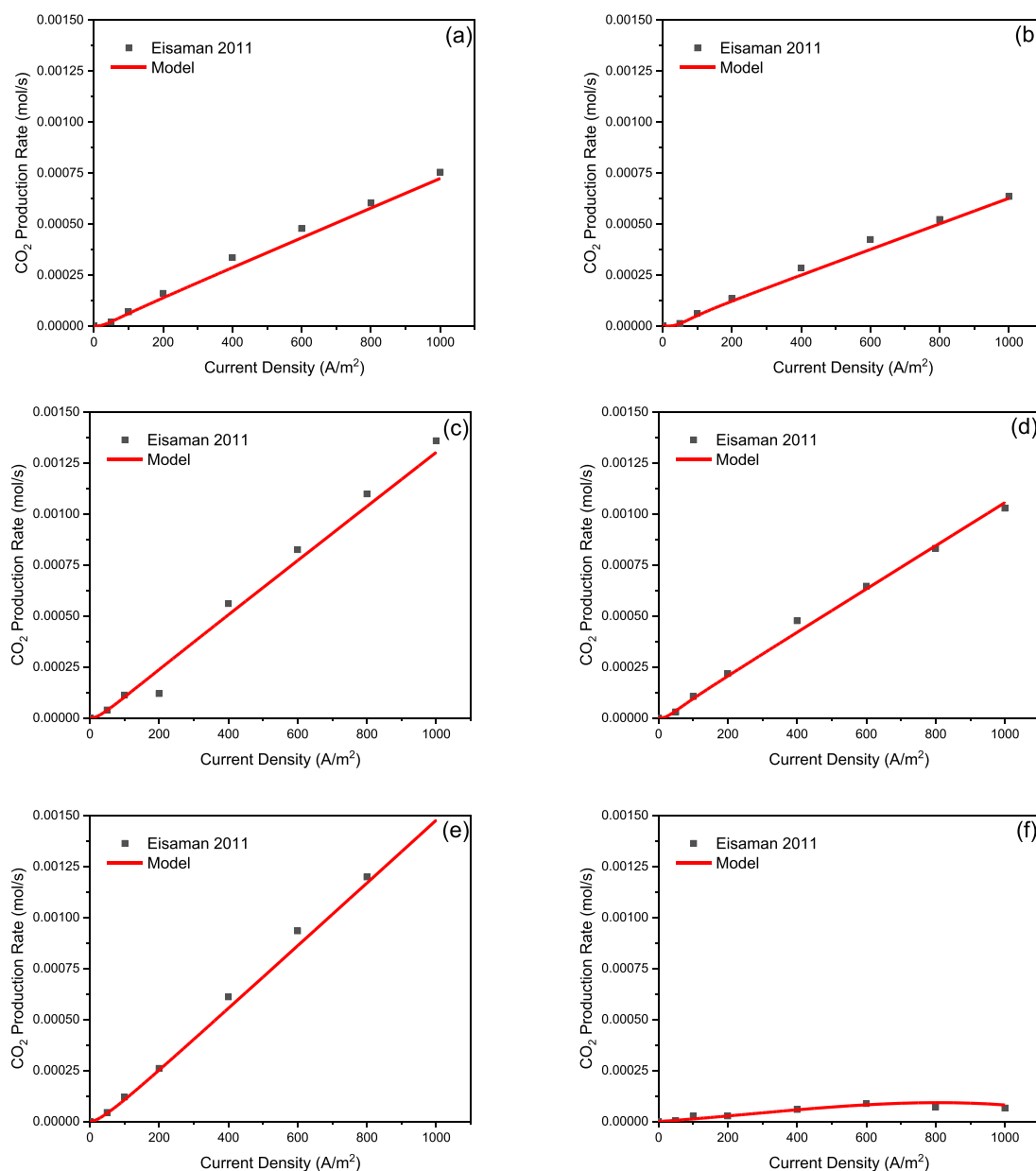


Figure 6. CO₂ production rate as a function of current density (black square) measured experimentally²⁰ and (red line) calculated with the BP MED model for (a) 0.5 M K₂CO₃, (b) 2 M K₂CO₃, (c) 0.25 M K₂CO₃ + 0.25 M KHCO₃, (d) 0.375 M K₂CO₃ + 0.125 M KHCO₃, (e) 0.5 M KHCO₃, and (f) 0.5 M K₂CO₃ + 0.1 M KOH-rich solutions.

the experimental results. The same behavior is observed for all the rich compositions. The energy demand presents a minimum at around 100 A/m² due to a trade-off between current efficiency and voltage drop. Indeed, at very low current densities, η is quite poor (Figure 4), while the voltage drop (and consequently the power consumption) across the BP MED cell increases with increasing i , as described by eq 12.

The composition affects the energy demand in different ways. First, it influences the current efficiency, as shown in Figure 4. The effect of efficiency is not as straightforward as it might seem, since for fast CO₂ production rates a larger amount of carbon dioxide bubbles is released, thus increasing the resistance of the cell. However, the composition also affects the solution conductivity which, in turn, determines the voltage drop across the cell. Indeed, the lower the electrical

conductivity of the rich solution is, the steeper will be the energy demand curve after the minimum.

As previously mentioned, at relatively high current densities, the fast CO₂ production rate can lead to the release of carbon dioxide in the form of bubbles. This results in an increased power consumption, as the resistance of the base compartment grows due to the presence of a nonconducting phase. This problem can be avoided by increasing the pressure at which the BP MED cell is operated. Indeed, the higher the pressure is, the higher the amount of CO₂ dissolved in the rich solutions is.

Eisaman et al.²¹ provided an experimental proof of concept of high-pressure BP MED. The results showed that at pressures higher than 6 atm the formation of carbon dioxide bubbles is prevented even at the highest supplied current density (1390 A/m²), thus providing a lower energy demand.

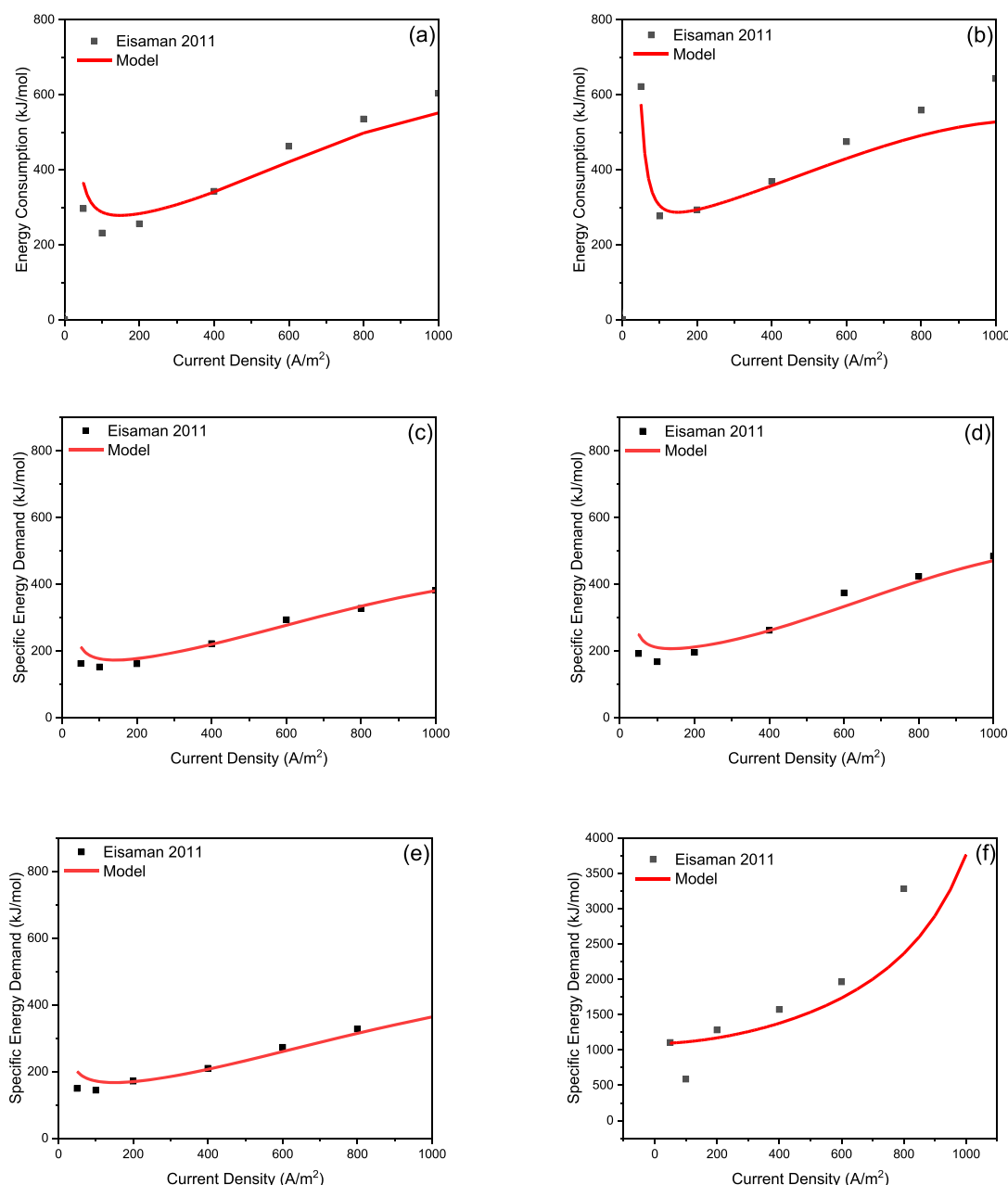


Figure 7. Specific energy demand as a function of current density (black square) measured experimentally²⁰ and (red line) calculated with the BPMED model for (a) 0.5 M K_2CO_3 , (b) 2 M K_2CO_3 , (c) 0.25 M K_2CO_3 + 0.25 M $KHCO_3$, (d) 0.375 M K_2CO_3 + 0.125 M $KHCO_3$, (e) 0.5 M $KHCO_3$, and (f) 0.5 M K_2CO_3 + 0.1 M KOH-rich solutions.

Figure 8 shows the specific energy demand measured by Eisaman et al. for the regeneration of a rich solution containing 0.5 M $KHCO_3$ carried out at 1 and 9 atm.^{20,21} The experimental results are compared to those computed with the BPMED model with and without the correction for the gas resistance, which are described with eqs 15 and 16. It can be noticed that when the CO_2 bubbles are not accounted for the model produces quite a good description of the energy demand of the high-pressure BPMED process. Therefore, Figure 8 also confirms that eqs 15 and 16 are necessary to provide an accurate representation of the performances of a low-pressure BPMED stack.

To conclude, the results reported previously show that the model is able to provide an adequate description of the performance of a BPMED stack in terms of the CO_2

production rate and specific energy demand. The model is adopted to assess the capital and operating costs of a large-scale electro dialysis unit. Eventual uncertainty regarding the current efficiency is taken into account through sensitivity analysis.

4.2. Assessment of Air Contactor Operating Conditions. CE claims to have designed and optimized the air contactor unit with the aim of minimizing the CO_2 capture cost. For this reason, in this analysis, the dimensions of the air contactor and the air velocity will be kept constant and equal to the values found by CE.

The equilibrium of the KOH – CO_2 – H_2O system has been studied with the help of the Aspen Plus thermodynamic model. Carbon dioxide can assume three different forms in a KOH aqueous solution: dissolved CO_2 ($CO_{2(l)}$), potassium carbo-

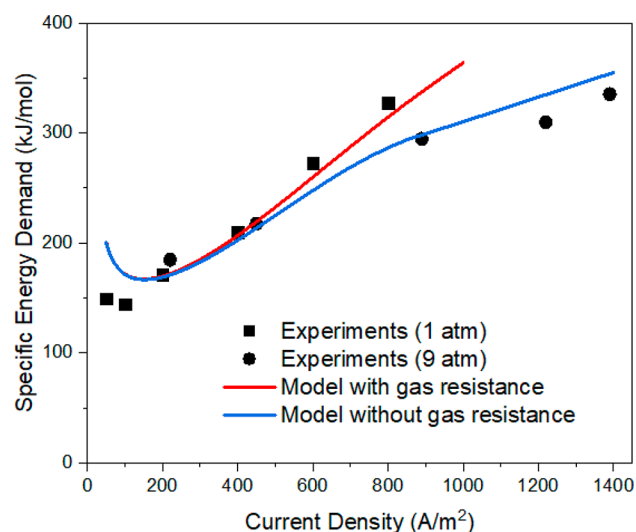


Figure 8. Specific energy demand as a function of current density for a 0.5 M KHCO_3 solution measured experimentally at (black square) 1 atm²⁰ and (black circle) 9 atm²¹ and calculated with the BPMED model (red line) with and (blue line) without gas resistance.

nate (K_2CO_3), and potassium bicarbonate (KHCO_3). The distribution of these species is governed by the pH of the system, as reported in Figure 9. In absorption processes, very

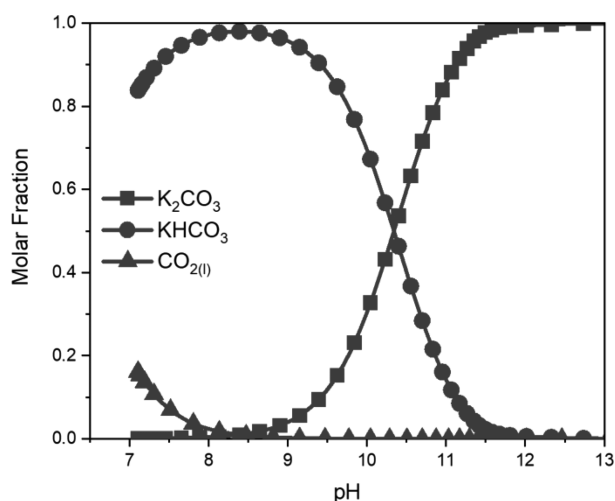


Figure 9. Distribution of carbonate species as a function of solution pH.

basic lean solutions are employed, as the rate of CO_2 capture decreases substantially with decreasing pH. Consequently, the concentration of KHCO_3 in the rich stream is usually negligibly small, the CO_2 assuming almost exclusively the form of K_2CO_3 . This is a major setback, as the results presented in the previous paragraph have shown that in BPMED the lowest energy demand and fastest CO_2 production rate are achieved with rich solutions containing exclusively potassium bicarbonate. Moreover, it has been shown that the presence of KOH has a detrimental effect on the current efficiency η . Therefore, the BPMED would perform best by adopting diluted, low-basicity lean streams. Since CO_2 capture and solvent regeneration are favored by opposite operating conditions, there is a trade-off between these two

processes. An optimization of the overall WS-BPMED process is, therefore, required.

To assess the performance of the air contactor unit and BPMED stack, two indicators have been selected and are defined below.

Carbonate Species Distribution Ratio:

$$\text{CSDR} = \frac{C_{\text{CO}_2(l)}^{\text{RICH}} + C_{\text{K}_2\text{CO}_3}^{\text{RICH}} + C_{\text{KHCO}_3}^{\text{RICH}}}{C_{\text{KOH}}^{\text{RICH}}} \quad (21)$$

CO_2 Recovery:

$$R_{\text{CO}_2} = \frac{F_{\text{CO}_2}^{\text{IN}} - F_{\text{CO}_2}^{\text{OUT}}}{F_{\text{CO}_2}^{\text{IN}}} \quad (22)$$

The carbonate species distribution ratio (CSDR) is defined as the ratio between the rich solution concentrations of the CO_2 -carrying components over the potassium hydroxide concentration. This is an important indicator, as it has been shown previously that the composition of the rich solution has a great influence on the efficiency of the BPMED regeneration process. This effect can be clearly discerned in Figure 10.

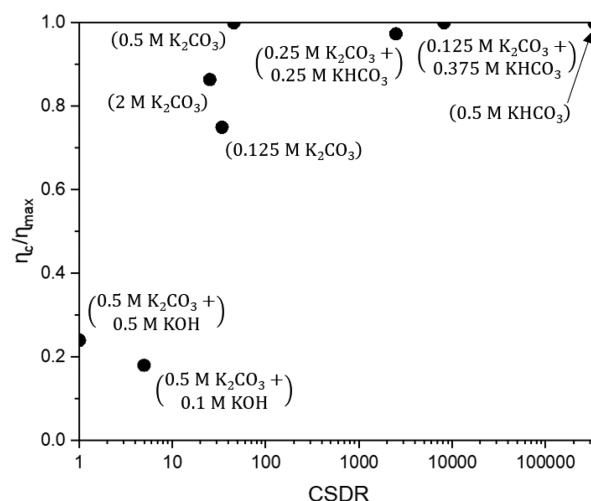


Figure 10. Ratio between the fitting parameter η_c and the maximum achievable efficiency η_{max} as a function of the CSDR for the rich solutions compositions assessed by Eisaman.²⁰

In this picture, the ratio η_c/η_{max} is reported as a function of the CSDR for the different rich solution compositions considered in this work. As already mentioned before, η_c is a parameter used in eq 19 and represents the asymptotic value reached by the efficiency at high current densities. Here, η_{max} is the maximum achievable efficiency, which is by definition equal to 1 for solutions containing exclusively KHCO_3 and 0.5 for solutions of K_2CO_3 . An average weighted on the concentration is adopted for solutions containing multiple ions. It can be observed that for low values of the CSDR the η_c/η_{max} ratio is well below 1, a value which is reached only for a CSDR of about 45. This means that to attain the highest possible efficiency effort must be taken to ensure that the CSDR is above this value. To identify an operating range which fulfills this requirement, a sensitivity analysis on the air contactor unit has been performed. This has been carried out through simulations with different lean compositions and liquid to gas ratios (L/G), defined as the ratio between the

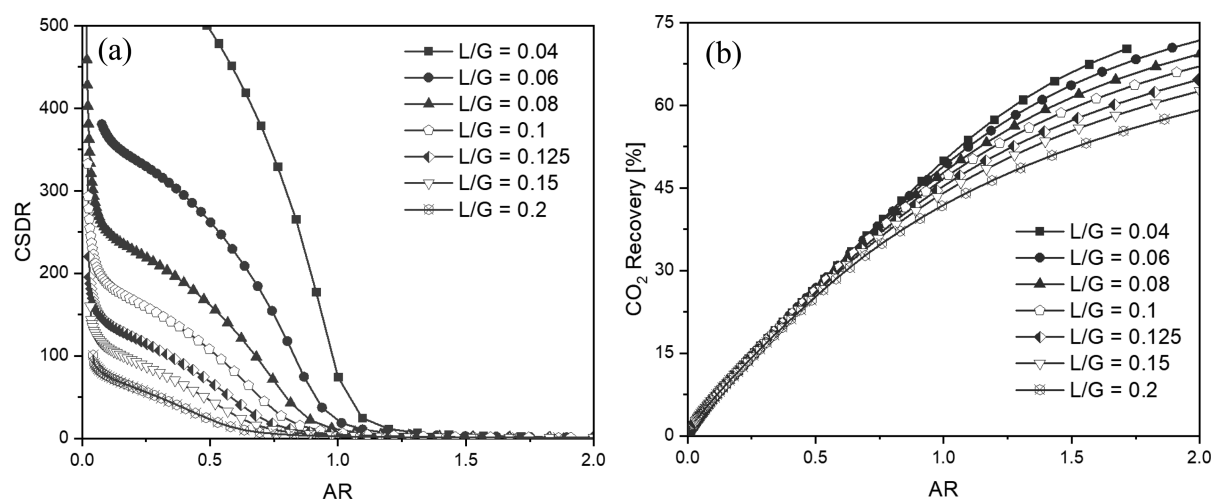


Figure 11. (a) CSDR and (b) CO₂ recovery as a function of the absorbent ratio (AR) for several liquid to gas ratios (L/G).

lean and air total mass flow rates. Figure 11a shows the results related to the CSDR as a function of the absorbent ratio (AR), which is defined as follows:

Absorbent Ratio:

$$AR = \frac{F_{KOH}^{LEAN}}{F_{CO_2}^{IN}} \quad (23)$$

It can be observed that high values of the CSDR can be achieved for an AR lower than 1. Indeed, in this condition, the amount of KOH fed with the lean stream is smaller than the amount of CO₂ present in the air stream. This means that very high conversions of potassium hydroxide to K₂CO₃ and KHCO₃ can be achieved, thus providing large CSDRs. From Figure 11a, it is also clear that for a fixed AR, CSDR increases with decreasing L/G. This is due to the lower KOH concentration that has to be set to achieve the same AR with a higher total flow rate. A more diluted lean stream provides slower absorption kinetics and, therefore, lower potassium hydroxide conversion.

This effect is even more apparent in Figure 11b, which reports the CO₂ recovery (R_{CO_2}) as a function of the AR. Here, R_{CO_2} describes the performances of the capture process, and it is strictly related to the cost of separating carbon dioxide from air. Since the air velocity is kept constant at the optimal value found by CE, a higher R_{CO_2} implies that a lower number of air contactor units is required to achieve the desired plant capacity, as a single unit is capable of capturing a greater amount of carbon dioxide. Figure 11b shows that the capture process is favored at high AR, whereas it has already been demonstrated that the solvent regeneration would be efficient only for small AR. This means that there exists a value of the AR that optimizes the overall performance of the process and, therefore, minimizes total capture costs.

Unfortunately, it was not possible to determine an exact relationship between the CSDR and the current efficiency from the data reported in Figure 10. For this reason, it was not possible to carry out a straightforward optimization of the process. Since it was shown before that the current efficiency η has a great influence on the energy demand of the BPMED process, it has been decided to prioritize the maximization of this parameter. The economic analysis that is presented in the next paragraph shows that this approach is justified.

The operating conditions which resulted from the analysis are reported in Table 2, together with the ones adopted by CE

Table 2. Optimal Air Contactor Operating Conditions for the BPMED Regeneration Process and Carbon Engineering Process

Process	WS-BPMED	Carbon Engineering ¹⁵
Air contactor		
Number of units	2660	1600
L/G	0.04	0.6
CO ₂ recovery, %	52.5	74.5
Lean stream		
KOH concentration, mol/m ³	0.368	1.1
K ₂ CO ₃ concentration, mol/m ³	0	0.45
Rich stream		
KOH concentration, mol/m ³	0.0053	1.075 ^a
K ₂ CO ₃ concentration, mol/m ³	0.217	0.475 ^a
KHCO ₃ concentration, mol/m ³	0.0014	0 ^a
CSDR	41	0.44

^aResults obtained from Aspen Plus simulation.

for their process. To achieve the desired capacity of 1 Mton-CO₂/yr, a remarkable increase in the number of air contactor units with respect to the CE process has been estimated. This was expected, as the chosen operating conditions do not favor the capture of carbon dioxide, as indicated by the lower CO₂ recovery. On the other hand, the CSDR assessed for the rich stream indicates that high current efficiencies could be achieved, thus ensuring lower energy demands for the BPMED.

4.3. Techno-Economic Assessment. A techno-economic assessment has been carried out with the aim of estimating the cost of carbon dioxide captured from a plant with a capacity of 1 MtonCO₂/yr. The BPMED model previously validated has been applied to assess the costs related to the regeneration of the sorbent using industrial-scale equipment. To account for uncertainties regarding the current efficiency, the assessment has been carried out for η of 40% and 50%, as we can be confident that a rich stream with the composition reported in Table 2 would provide an efficiency in this range. The electrodialysis stack and the membranes are based on

commercially available products.³⁵ The main parameters used for the cost analysis are reported in Table 3.

Table 3. Main Assumptions Used for the Techno-Economic Assessment

Parameter	Value	Justification
Number of cells	2400	Value reported by Iizuka et al. ¹⁹
Membrane area, m ²	1.785	Value reported by Iizuka et al. ¹⁹
δ , mm	1.5	Assumption based on values reported by Tanaka ³⁶
BPM cost, \$/m ²	750	Value reported by Iizuka et al. ¹⁹
AEM cost, \$/m ²	75	Assumed to be 1/10th of BPM cost as in Jiang et al. ³⁷
Stack cost, M\$/unit	1	Assumption based on values reported by Tanaka ³⁶
Electricity cost, \$/kWh	0.06	Value reported by Keith et al. ¹⁵

As shown in Figure 7, the specific energy demand presents an optimum with respect to the current density due to a trade-off between efficiency and voltage drop across the stack. This behavior is also reflected in the operating costs of the WS-BPMED process, as reported in Figure 12a. As a matter of fact, the power consumption of the electrodialysis units comprises more than half of the levelized OPEX, which is broken down in Table 4. It should be pointed out, however, that the electrodialysis regeneration is not necessarily an energy intensive process. The results obtained from the BPMED model show that by employing low current densities the regeneration could be carried out with only 236 kJ/mol-CO₂, which is considerably lower than the 338 kJ/mol-CO₂ we estimated is required for the thermochemical cycle designed by CE.²⁴ Unfortunately, at low current densities, the CO₂ production rate is very slow, as described by eq 11. This implies that the lower the current density is, the larger is the required membrane area to achieve the desired capacity. Figure 12b clearly shows this effect, as the levelized CAPEX steadily decreases with current density i .

The higher membrane area requirement, however, also affects the operating costs. Indeed, as reported in Table 4, the membrane replacement accounts for almost the entirety of the fixed operation and maintenance costs which, in turn, comprise almost half of the levelized OPEX. Consequently, the capture cost is minimized at relatively high current densities, as shown in Figure 12. Although optimal from an economic point of view, these conditions are energetically unfavorable, as the energy demand reaches a value of 957 kJ/mol. In these conditions, for the process to achieve negative emissions, only

low carbon intensity energy sources should be used. Employing natural gas or coal would result in net positive CO₂ emissions.³⁸

The high power consumption of the BPMED stacks, combined with the large membrane cost, makes this process extremely expensive. It can be observed from Figure 12c that the minimum capture cost is around 773 \$/ton-CO₂, significantly larger than the estimates of CE (Table 4).

Due to the large impact of membrane and energy costs on the process economics, a sensitivity analysis on the major membrane-related parameters and on the electricity cost has been carried out. The aim is to assess whether a future reduction in the price of BPM, AEM, or renewable energy could make the WS-BPMED process more attractive and competitive. The results are shown in Figure 13 and are compared to scenario A of CE's process, in which the energy demand is entirely met with natural gas.¹³ For each of the three analyses, only the sensitivity parameter is changed, while the other parameters are kept at their base-case values, which are reported in Table 3.

It can be observed that membrane lifetime and electricity cost are the most influential parameters. This was expected, as membrane replacement and BPMED power consumption make up most of the OPEX which, in turn, comprises the majority of the capture cost.

Unfortunately, in no investigated condition is the WS-BPMED process more cost-effective than CE's process. This means that significant developments in membrane technology and a decrease in electricity cost have both to take place for the proposed process to be the most efficient. Efforts should especially be made to increase the lifetime of the membranes from the current value of roughly 3 years,³¹ as this improvement would have a tremendous influence on the capture cost. Even though the results reported in Figure 13 show that the WS-BPMED process is still far from being economically viable, it does not mean that it will never be. Indeed, in the coming years, a further reduction of the renewable energy price can be expected, with estimates as low as 0.018 \$/kWh by 2050.³⁹ It is also reasonable to assume that by 2050 cheaper and more resistant membranes would be produced. Moreover, further improvements in the process could also be investigated, which are highlighted in the next section.

5. DISCUSSION

The biggest challenge associated with the WS-BPMED process is without a doubt the optimal integration of capture and

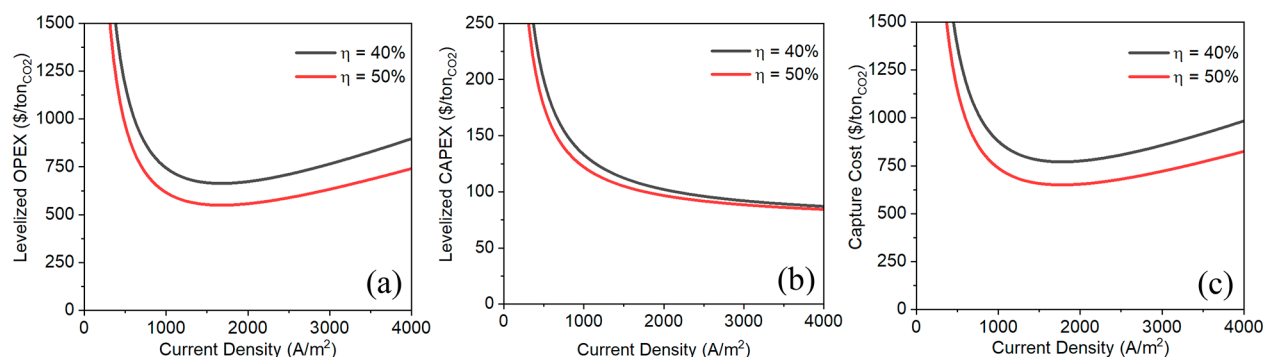


Figure 12. (a) Levelized OPEX, (b) levelized CAPEX, and (c) capture cost for the base case scenario as a function of the current density.

Table 4. Economic Evaluation of the WS-BPMED Process and Comparison with CE DAC Process

Process	WS-BPMED	Carbon Engineering ¹⁵
Bare erected cost [M\$]		
Air contactors	185.6	114.2
BPMED stacks	21.91 ^a	—
Membranes	86.25 ^a	—
Pellet reactor	—	76.9
Calcliner slaker	—	43.8
CO ₂ compressor	24.2 ^b	17.2
Other equipment	4.325 ^b	191.9
Total	322.3	444
TOC × CCF, M\$/y	106.5	140.85
Levelized fixed O&M [\$/ton-CO₂]		
Membrane replacement	248.6 ^a	—
Stack replacement	7.02 ^a	—
Labor, insurance, maintenance	36.67	11.16
Total	292.3	11.16
Levelized variable O&M [\$/ton-CO₂]		
Air contactor fan energy	3.66	3.66
CO ₂ compression	6.84	7.92
BPMED energy	363.5 ^a	—
Total electricity input	374	—
Total natural gas input	—	30.84
Capture cost, \$/ton-CO ₂	773 ^a	232

^aMean between costs estimated at 40% and 50% η . ^bCalculated with Aspen Plus.

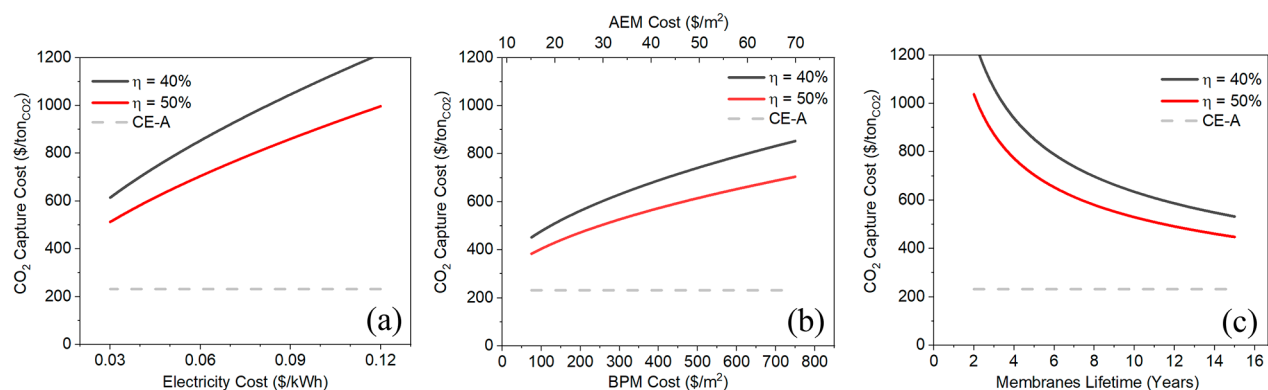


Figure 13. Sensitivity analysis of the CO₂ capture cost to (a) electricity cost, (b) membranes cost, and (c) membranes lifetimes for the WS-BPMED process and scenario A from CE.¹⁵

regeneration. With the current state of ion-exchange membranes technology and renewable energy price, it might not be possible to achieve a competitive price. However, a potential solution has been reported in the literature.¹⁶ As previously explained, the equilibrium of the KOH–H₂O–CO₂ system is strongly dependent on the pH, with basic solutions resulting in the formation of potassium carbonate. The addition of a weak acid to the rich solution would cause a reduction of the pH and, consequently, the conversion of K₂CO₃ to KHCO₃, which is much more efficiently and quickly regenerated through BPMED. This method has been proven experimentally for different amines;^{40,41} however, the separation and recovery of the acids is still an open question. An alternative could be provided by monovalent-ion-selective membranes. These membranes are able to separate monovalent ions from a solution containing both monovalent and multivalent ions.⁴² Several methods to tune the ion selectivity

are available,⁴³ with the application of a thin, oppositely charged layer being the one presenting the best results. The electrostatic repulsion between ions and the layer hinders the permeation of multivalent ions more effectively than for monovalent ions, thus making the membrane selective. The adoption of monovalent-ion-selective AEMs could improve the process efficiency since the transport of HCO₃[−] ions would be favored.

The costs related to ion-exchange membranes have a great impact on the process economics. In the literature, several interesting developments that could reduce the expenses associated with membranes are reported. Ion-exchange membranes are generally made of polymers containing functional groups that allow the permeation of cations or anions. It has been observed that the addition of functional inorganic particles to the polymer phase improves the thermal and mechanical stability.⁴⁴ Membranes with such a structure

are called mixed matrix membranes (MMMs). Polymer blending is another simple but promising way to rectify the shortcomings of single components.⁴⁵ It consists of mixing two different kinds of polymers in an appropriate ratio to create a material that combines the advantages of each polymer while overcoming their defects. In addition to the synthesis of new materials, the development of adequate membrane preparation methods is of great importance in achieving cost effectiveness. Several novel methods have been described in the literature, which might provide improved stability at a lower cost.⁴⁵

Segmented bipolar membranes (SBPMs), which can transport ions and split water at the same time,⁴⁶ could dramatically decrease the cost of the WS-BPMED process, as they would provide better pH control and make the AEMs unnecessary.

The results presented in this work have shown that the WS-BPMED process is currently unable to compete with other DAC processes. However, further developments in membrane technology or better process design could change this. There are also other advantages of electrodialysis regeneration, such as that it allows complete electrification of the process, has fast ramp up times, and avoids solids handling. These could be key advantages for giga-ton deployment. Finally, BPMED is a flexible technology that could be efficiently employed at different scales.

6. CONCLUSIONS

The process described in this work combines CO₂ capture from air through a proven and cost-effective wet scrubbing unit with solvent regeneration by means of bipolar-membrane electrodialysis. This process, referred to as WS-BPMED, was studied and compared with the reference DAC technology developed by CE from a techno-economic point of view.

A MATLAB model has been developed and validated to describe the performance of the BPMED stack, while Aspen Plus has been adopted to simulate the wet scrubbing unit. It has been found that CO₂ capture and solvent regeneration are favored by opposite conditions in terms of lean stream composition. There is, therefore, a trade-off between these two operations. The optimization has been carried out on the basis of a sensitivity analysis on the air contactor unit and on considerations arising from the BPMED model. It has been shown that current efficiencies close to the maximum one can be achieved with a tolerable decline in the performance of the air contactor. The techno-economic analysis showed that the WS-BPMED process is presently too expensive. The estimated capture cost is 773 \$/ton-CO₂, more than 3 times higher than the cost estimated by CE for their process.

■ ASSOCIATED CONTENT

Supporting Information

The Supporting Information is available free of charge at <https://pubs.acs.org/doi/10.1021/acs.iecr.9b05641>.

Additional parameters used in the BPMED model and Aspen flowsheet and assumptions related to the calculation of capture costs (PDF)

■ AUTHOR INFORMATION

Corresponding Author

Martin van Sint Annaland – Department of Chemical Engineering and Chemistry, Technische Universiteit Eindhoven, 5600, MB, Eindhoven, The Netherlands; orcid.org/0000-0002-2903-7443; Email: m.v.sintannaland@tue.nl

Authors

Francesco Sabatino – Department of Chemical Engineering and Chemistry, Technische Universiteit Eindhoven, 5600, MB, Eindhoven, The Netherlands

Mayank Mehta – Department of Chemical Engineering and Chemistry, Technische Universiteit Eindhoven, 5600, MB, Eindhoven, The Netherlands

Alexa Grimm – Copernicus Institute of Sustainable Development, Universiteit Utrecht, 3584, CB, Utrecht, The Netherlands

Matteo Gazzani – Copernicus Institute of Sustainable Development, Universiteit Utrecht, 3584, CB, Utrecht, The Netherlands; orcid.org/0000-0002-1352-4562

Fausto Gallucci – Department of Chemical Engineering and Chemistry, Technische Universiteit Eindhoven, 5600, MB, Eindhoven, The Netherlands

Gert Jan Kramer – Copernicus Institute of Sustainable Development, Universiteit Utrecht, 3584, CB, Utrecht, The Netherlands

Complete contact information is available at:

<https://pubs.acs.org/10.1021/acs.iecr.9b05641>

Notes

The authors declare no competing financial interest.

■ ACKNOWLEDGMENTS

This work was sponsored by Shell Global Solutions International BV.

■ REFERENCES

- (1) Allen, M.; Dube, O. P.; Solecki, W.; Aragón-Durand, F.; Cramer, W.; Humphreys, S.; Kainuma, M.; Kala, J.; Mahowald, N.; Mulugetta, Y.; et al. *Global Warming of 1.5°C*; An IPCC Special Report on the Impacts of Global Warming of 1.5°C above Pre-Industrial Levels and Related Global Greenhouse Gas Emission Pathways, in the Context of Strengthening the Global Response to the Threat of Climate Change, Sustainable Development, And Efforts to Eradicate Poverty; IPPC, 2018.
- (2) Fuss, S.; Lamb, W. F.; Callaghan, M. W.; Hilaire, J.; Creutzig, F.; Amann, T.; Beringer, T.; de Oliveira Garcia, W.; Hartmann, J.; Khanna, T. Negative Emissions - Part 2: Costs, Potentials and Side Effects. *Environ. Res. Lett.* **2018**, *13*, 2–4.
- (3) Lackner, K. S.; Ziock, H.; Grimes, P. *Carbon Capture from Air, Is It an Option?* 24th Annual Technical Conference on Coal Utilization and Fuel Systems, Clearwater, FL, USA, 03/08/1999–03/11/1999.
- (4) Carey, R.; Gomezplata, A.; Sarich, A. An Overview into Submarine CO₂ Scrubber Development. *Ocean Eng.* **1983**, *10* (4), 227–233.
- (5) Lackner, K. S. The Thermodynamics of Direct Air Capture of Carbon Dioxide. *Energy* **2013**, *50* (1), 38–46.
- (6) Keith, D. W.; Heidel, K.; Cherry, R. Capturing CO₂ from the Atmosphere: Rationale and Process Design Considerations. In *Geo-Engineering Climate Change: Environmental Necessity or Pandora's Box?*; Thompson, J. M. T., Launder, B., Eds.; Cambridge University Press, 2010; pp 107–126.
- (7) Sanz-Pérez, E. S.; Murdock, C. R.; Didas, S. A.; Jones, C. W. Direct Capture of CO₂ from Ambient Air. *Chem. Rev.* **2016**, *116* (19), 11840–11876.
- (8) Li, H.; Wang, K.; Sun, Y.; Lollar, C. T.; Li, J.; Zhou, H. C. Recent Advances in Gas Storage and Separation Using Metal–Organic Frameworks. *Mater. Today* **2018**, *21* (2), 108–121.
- (9) Didas, S. A.; Choi, S.; Chaikittisilp, W.; Jones, C. W. Amine-Oxide Hybrid Materials for CO₂ Capture from Ambient Air. *Acc. Chem. Res.* **2015**, *48* (10), 2680–2687.
- (10) Veselovskaya, J. V.; Derevschikov, V. S.; Kardash, T. Y.; Stonkus, O. A.; Trubitsina, T. A.; Okunev, A. G. Direct CO₂ Capture

from Ambient Air Using K_2CO_3/Al_2O_3 Composite Sorbent. *Int. J. Greenhouse Gas Control* **2013**, *17*, 332–340.

(11) Lackner, K. S. Capture of Carbon Dioxide from Ambient Air. *Eur. Phys. J.: Spec. Top.* **2009**, *176* (1), 93–106.

(12) Zeman, F. Energy and Material Balance of CO_2 Capture from Ambient Air. *Environ. Sci. Technol.* **2007**, *41* (21), 7558–7563.

(13) Baciocchi, R.; Storti, G.; Mazzotti, M. Process Design and Energy Requirements for the Capture of Carbon Dioxide from Air. *Chem. Eng. Process.* **2006**, *45* (12), 1047–1058.

(14) Socolow, R.; Desmond, M.; Aines, R.; Blackstock, J.; Bolland, O.; Kaarsberg, T.; Lewis, N.; Mazzotti, M.; Pfeiffer, A.; Sawyer, K.; Sirola, J.; Smit, B.; Wilcox, J. *Direct Air Capture of CO_2 with Chemicals*; A Technology Assessment for the APS Panel on Public Affairs; American Physical Society, Panel on Public Affairs, June 1, 2011.

(15) Keith, D. W.; Holmes, G.; St. Angelo, D.; Heidel, K. A Process for Capturing CO_2 from the Atmosphere. *Joule* **2018**, *2*, 1573–1594.

(16) Li, T.; Keener, T. C. A Review: Desorption of CO_2 from Rich Solutions in Chemical Absorption Processes. *Int. J. Greenhouse Gas Control* **2016**, *51*, 290–304.

(17) Zabolotskii, V.; Sheldeshov, N.; Melnikov, S. Heterogeneous Bipolar Membranes and Their Application in Electrodialysis. *Desalination* **2014**, *342*, 183–203.

(18) Nagasawa, H.; Yamasaki, A.; Iizuka, A.; Kumagai, K.; Yanagisawa, Y. A New Recovery Process of Carbon Dioxide from Alkaline Carbonate Solution via Electrodialysis. *AIChE J.* **2009**, *55* (12), 3286–3293.

(19) Iizuka, A.; Hashimoto, K.; Nagasawa, H.; Kumagai, K.; Yanagisawa, Y.; Yamasaki, A. Carbon Dioxide Recovery from Carbonate Solutions Using Bipolar Membrane Electrodialysis. *Sep. Purif. Technol.* **2012**, *101*, 49–59.

(20) Eisaman, M. D.; Alvarado, L.; Larner, D.; Wang, P.; Garg, B.; Littau, K. A. CO_2 Separation Using Bipolar Membrane Electrodialysis. *Energy Environ. Sci.* **2011**, *4* (4), 1319–1328.

(21) Eisaman, M. D.; Alvarado, L.; Larner, D.; Wang, P.; Littau, K. A. CO_2 Desorption Using High-Pressure Bipolar Membrane Electrodialysis. *Energy Environ. Sci.* **2011**, *4* (10), 4031.

(22) Eisaman, M. D.; Parajuly, K.; Tuganov, A.; Eldershaw, C.; Chang, N.; Littau, K. A. CO_2 Extraction from Seawater Using Bipolar Membrane Electrodialysis. *Energy Environ. Sci.* **2012**, *5* (6), 7346–7352.

(23) Eisaman, M. D.; Schwartz, D. E.; Amic, S.; Larner, D. L.; Zesch, J.; Torres, F.; Littau, K. *Energy-Efficient Electrochemical CO_2 Capture from the Atmosphere*; Technical Proceedings of the 2009 Clean Technology Conference and Trade Show, Houston, TX, May 3–7, 2009.

(24) Sabatino, F.; Gazzani, M.; Grimm, A.; Gallucci, F.; van Sint Annaland, M.; Kramer, G. J. Comparative Assessment and Optimization of Direct Air Capture via Absorption and Adsorption Processes. Poster session presented at International Conference on Negative CO_2 Emissions, Göteborg, Sweden, May 22–24, 2018.

(25) Astarita, G.; Savage, D. W.; Longo, J. M. Promotion of CO_2 Mass Transfer in Carbonate Solutions. *Chem. Eng. Sci.* **1981**, *36* (3), 581–588.

(26) Stolaroff, J. K.; Keith, D. W.; Lowry, G. V. Carbon Dioxide Capture from Atmospheric Air Using Sodium Hydroxide Spray. *Environ. Sci. Technol.* **2008**, *42* (8), 2728–2735.

(27) Holmes, G.; Keith, D. W. An Air-Liquid Contactor for Large-Scale Capture of CO_2 from Air. *Philos. Trans. R. Soc., A* **2012**, *370* (1974), 4380–4403.

(28) Holmes, G.; Nold, K.; Walsh, T.; Heidel, K.; Henderson, M. A.; Ritchie, J.; Klavins, P.; Singh, A.; Keith, D. W. Outdoor Prototype Results for Direct Atmospheric Capture of Carbon Dioxide. *Energy Procedia* **2013**, *37*, 6079–6095.

(29) Henderson, M. A.; Keith, D. W.; Kainth, A. P. S.; Heidel, K. R.; Ritchie, J. A. Target Gas Capture. US Patent US 8,871,008 B2, 2014.

(30) *Rate-Based Model of the CO_2 Capture Process by K_2CO_3 Using Aspen Plus*; Aspen Technology, 2013.

(31) Tanaka, Y. Bipolar Membrane Electrodialysis. *Ion Exch. Membr.* **2015**, *1956*, 369–392.

(32) Nielsen, L. E. The Thermal and Electrical Conductivity of Two-Phase Systems. *Ind. Eng. Chem. Fundam.* **1974**, *13* (1), 17–20.

(33) Jorissen, J.; Simmrock, K. H. The Behaviour of Ion Exchange Membranes in Electrolysis and Electrodialysis of Sodium Sulphate. *J. Appl. Electrochem.* **1991**, *21* (10), 869–876.

(34) Spallina, V.; Pandolfo, D.; Battistella, A.; Romano, M. C.; van Sint Annaland, M.; Gallucci, F. Techno-Economic Assessment of Membrane Assisted Fluidized Bed Reactors for Pure H_2 Production with CO_2 Capture. *Energy Convers. Manage.* **2016**, *120*, 257–273.

(35) Asahi Glass Co. Products Catalogue. Selemion Ion Exchange Membranes. <https://www.amp-ionex.com/products/selemion/pdf/selemion.pdf> (accessed May 9, 2019).

(36) Tanaka, Y. Electrodialysis. In *Ion Exchange Membranes*, Vol. 12; Elsevier, 2015; pp 255–293.

(37) Jiang, C.; Wang, Y.; Xu, T. An Excellent Method to Produce Morpholine by Bipolar Membrane Electrodialysis. *Sep. Purif. Technol.* **2013**, *115*, 100–106.

(38) Moomaw, W.; Burgherr, P.; Heath, G.; Lenzen, M.; J. Nyboer, A. V. Annex II: Methodology. In *IPCC Special Report on Renewable Energy Sources and Climate Change Mitigation*; Cambridge University Press, 2007; pp 195–209.

(39) Mayer, J. N. *Current and Future Cost of Photovoltaics: Long-Term Scenarios for Market Development, System Prices and LCOE of Utility-Scale PV Systems*; Agora Energiewende, 2015.

(40) Du, M.; Feng, B.; An, H.; Liu, W.; Zhang, L. Effect of Addition of Weak Acids on CO_2 Desorption from Rich Amine Solvents. *Korean J. Chem. Eng.* **2012**, *29* (3), 362–368.

(41) Feng, B.; Du, M.; Dennis, T. J.; Anthony, K.; Perumal, M. J. Reduction of Energy Requirement of CO_2 Desorption by Adding Acid into CO_2 -Loaded Solvent. *Energy Fuels* **2010**, *24* (1), 213–219.

(42) Güler, E.; van Baak, W.; Saakes, M.; Nijmeijer, K. Monovalent-Ion-Selective Membranes for Reverse Electrodialysis. *J. Membr. Sci.* **2014**, *455*, 254–270.

(43) Luo, T.; Abdu, S.; Wessling, M. Selectivity of Ion Exchange Membranes: A Review. *J. Membr. Sci.* **2018**, *555* (March), 429–454.

(44) Bakangura, E.; Wu, L.; Ge, L.; Yang, Z.; Xu, T. Mixed Matrix Proton Exchange Membranes for Fuel Cells: State of the Art and Perspectives. *Prog. Polym. Sci.* **2016**, *57*, 103–152.

(45) Ran, J.; Wu, L.; He, Y.; Yang, Z.; Wang, Y.; Jiang, C.; Ge, L.; Bakangura, E.; Xu, T. Ion Exchange Membranes: New Developments and Applications. *J. Membr. Sci.* **2017**, *522*, 267–291.

(46) Kattan Rendi, O. M.; Kuenen, H. J.; Zwijnenberg, H. J.; Nijmeijer, K. Novel Membrane Concept for Internal pH Control in Electrodialysis of Amino Acids Using a Segmented Bipolar Membrane (SBPM). *J. Membr. Sci.* **2013**, *443*, 219–226.